

Improvement of resistive switching property in a noncrystalline and low-resistance $\text{La}_{0.7}\text{Ca}_{0.3}\text{MnO}_3$ thin film by using an Ag–Al alloy electrode

Weidong Yu, Xiaomin Li, Yang Rui, Xinjun Liu, Qun Wang and Lidong Chen

State Key Laboratory of High Performance Ceramics & Superfine Microstructure, Shanghai Institute of Ceramics, Chinese Academy of Sciences, 1295 Ding Xi Road, Shanghai 200050, People's Republic of China

E-mail: ywd2003@mail.sic.ac.cn

Received 17 May 2008, in final form 28 August 2008

Published 15 October 2008

Online at stacks.iop.org/JPhysD/41/215409

Abstract

A noncrystalline, low-resistance $\text{La}_{0.7}\text{Ca}_{0.3}\text{MnO}_3$ (LCMO) thin film was deposited by pulsed laser deposition at the substrate temperature of 550 °C and the oxygen pressure of 1 Pa. The low resistance of the resultant film was derived from the large leakage current due to the noncrystallinity of the LCMO film. Ag, Al and Ag–50%Al alloy metals were selected as top electrodes (TEs) on the LCMO film with a Pt bottom electrode to form Ag, Al, Ag–50%Al/LCMO/Pt multilayer units. It was found that stable bipolar resistive switching was only obtained in Al–50%Ag/LCMO/Pt units. Obvious hysteresis and ‘current leaps’ phenomena occurred clearly in I – V curves of high original resistance units with an Al–50%Ag TE. The low original resistance units can be turned to high resistance by a voltage sweep. Based on these results, a model was proposed to explain the switching properties of the Al–50%Ag/LCMO/Pt units, which will be helpful to improve the switching uniformity of RRAM devices.

1. Introduction

Electric-pulse-induced resistance (EPIR) switching [1–6] based on perovskite manganites $\text{Re}_{1-x}\text{A}_x\text{MnO}_3$ (Re = rare earth ions, A = Alkaline ions, $x = 0.3$ – 0.7) has attracted considerable interest for potential applications in next generation nonvolatile memory devices known as resistance random access memory (RRAM) [7]. Compared with other nonvolatile memories, RRAM has several advantages, such as fast erasing times, high densities and low operating power. The selected manganites for EPIR investigation are $\text{Pr}_{0.7}\text{Ca}_{0.3}\text{MnO}_3$ (PCMO) and $\text{La}_{0.7}\text{Ca}_{0.3}\text{MnO}_3$ (LCMO). It has been the consensus that the films for EPIR investigation must possess high original resistance (HOR > 1 k Ω) to maintain a large electrical field during the pulse despite their intrinsic low resistances by polarons conduction. Recently, remarkable bipolar resistive switching has been found in an

Ag paste/ $\text{Pr}_{0.7}\text{Ca}_{0.3}\text{MnO}_3$ /Pt structure, in which the PCMO thin film has high crystallinity and low original resistance (LOR) [8]. The authors suggested that the function of the Ag point contact is similar to those of the previously proposed filament path and the nanodomain switch. Similar results have also been shown and discussed in our previous papers [3, 9]. But the Ag paint printing method was only adopted in the laboratory for academic research rather than the practical CMOS technology. Based on the previous study of Ag paste, we developed a novel electrode material to improve the switching properties of LOR films.

According to the published studies, several metal materials have been employed as top electrodes (TEs) for EPIR studies, such as Ag, Al, Ti, Mo and Au [1, 10–17]. No studies report that using these electrodes can achieve a stable EPIR switching in LOR oxide films (LOR < 1 k Ω) or improve the uniformity of the switching properties of high-resistance

LCMO or PCMO films. For the HOR TE/manganite unit, in which the manganite film possesses uniform electrical properties (no serious leakage current channels), all the above-mentioned TEs can guide the EPIR property of manganite units. But for LOR units with the manganite film electrically controlled by leakage channels, a direct contact between inert metal (Ag, Mo, Au) electrodes and manganite film occurred. The leakage channels still remain in the LOR units to hinder their EPIR effect. However, for active metal (Al, Ti) electrodes [15–17], it has been verified that a dense insulative oxide (AlO_x) layer was formed between the Al electrode and the manganite film [18], which will block the leakage channels to increase the resistance of the LOR units. The thickness of the AlO_x layer is variable and can increase with the magnitude and the numbers of electrical pulse above a certain threshold voltage. A too thick AlO_x layer can prevent the injection of the electrons to irreversibly increase the resistance of the units. On the other hand, it is well known that the current leakage channels generally exist in the oxide films, even epitaxial thin films, due to uncontrollable factors (impurities, parameter fluctuation, etc) during actual film preparation, which seriously deteriorates the electrical uniformity. So it is essential to find an effective way of avoiding the influence of the current leakage besides enhancing the density and crystalline quality of the film by optimizing the growth process.

In this paper, a noncrystalline and low-resistance LCMO thin film was chosen to validate the favourable effect of Al–Ag alloy electrodes on the resistance switching of the manganite films. Besides the large chemical activity difference between Ag and Al (the electronegativity of Al: 1.61 and Ag: 1.93, respectively), the approximative work function (~ 4.2 eV) of Ag and Al, which ensures a similar interface barrier between the TE and the LCMO film, is another important reason to choose them for electrode alloying. The Al and Ag atomic ratio of 1 : 1 (Al–50%Ag) was selected. Pure Al and Ag were prepared with the same deposition condition for comparison. Besides the above purposes, this work has also provided a referential clue for understanding the EPIR mechanism.

2. Experiment

The $\text{La}_{0.7}\text{Ca}_{0.3}\text{MnO}_3$ film was prepared by pulse laser deposition on the Pt/Ti/SiO₂/Si substrate [19]. The laser deposition was carried out with a deposition rate of 1.5 nm min^{-1} by a pulse energy of 200 mJ. During the deposition, the substrate was maintained at 550°C , and the O₂ pressure was kept at 1 Pa. The thickness of the LCMO film is around 200 nm. Compared with the Ca content in the target, the deviation of the doped Ca content in the resultant film is $\pm 15\%$ measured by XPS and $\pm 10\%$ by EPMA, respectively, which are involved in the precision ranges of the XPS and EPMA. Al and Ag layers were, respectively, deposited by electron beam evaporation and thermal evaporation under a base vacuum of $< 5 \times 10^{-4}$ Pa and a substrate temperature of 200°C . The Al–50%Ag alloy layer was fabricated by simultaneously employing the above procedures with the same deposition rate to keep the Al and Ag atomic ratio of 1 : 1. The thicknesses of Al, Ag and Al–50%Ag layers were 200 nm

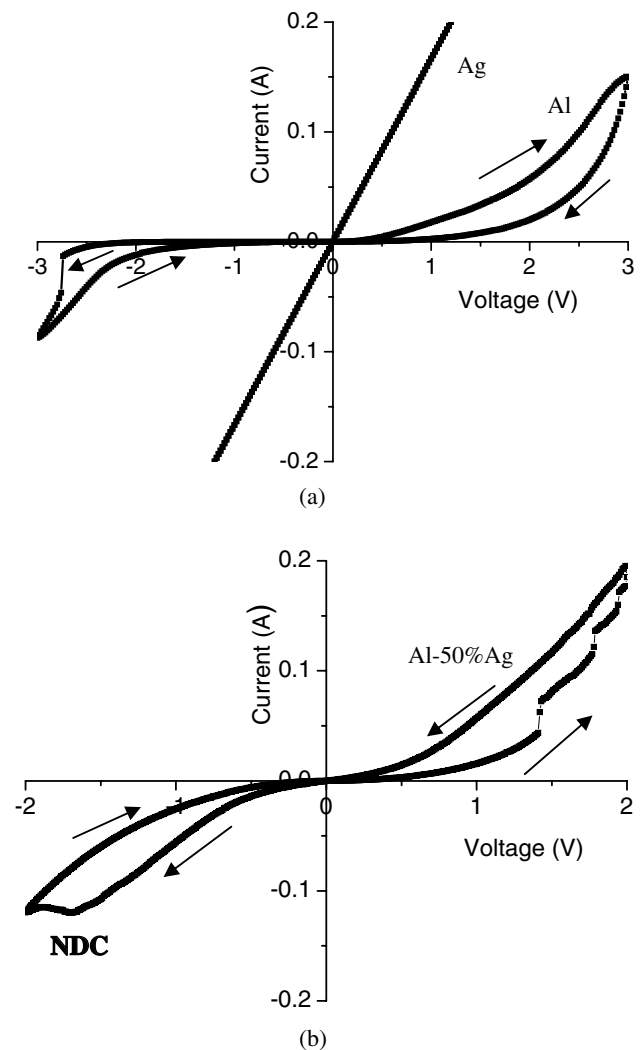


Figure 1. I – V characteristics of TEs/LCMO/Pt layered structures with Ag, Al TEs (a) and Al–50%Ag alloy TE (b). For Al TE, the current shown under positive voltage sweep was $100\times$ magnification of the actual value.

and their areas were 0.01 mm^2 . The resistance and I – V characteristics were measured with the standard two-wire I – V curve method. The electrical pulse was applied with a bias of 10 V and a constant pulse width of $10 \mu\text{s}$.

3. Results and discussion

Field emission scanning electron microscopy observation indicated that the obtained LCMO film is smooth, crack-free and homogeneous in thickness. The noncrystalline characteristic of the LCMO film was deduced from the x-ray diffraction curve, in which no obvious peaks were found. The noncrystallinity of LCMO results from the low substrate temperature and high oxygen pressure during film deposition, which remarkably decreases the active energy of the particles arriving on the substrate.

Figure 1 shows the I – V behaviours of the units with the TEs of Al, Ag, Al–50%Ag alloy, respectively. The voltages for Al–50% Ag electrodes were scanned as

$0 \rightarrow +2\text{ V} \rightarrow 0 \rightarrow -2\text{ V} \rightarrow 0$ and those for Al electrodes were $0 \rightarrow +3\text{ V} \rightarrow 0 \rightarrow -3\text{ V} \rightarrow 0$. The other measurement parameters are the same. It can be found that a linear I - V curve is obtained from Ag/LCMO/Pt units, as shown in figure 1(a). The Schottky contact between Ag (Work function = 4.2 eV) and LCMO (electron affinity = 4.9 eV) [1] has not been acquired, predicting the intrinsic LOR property of the LCMO film. The ohm-like contact between Ag and LCMO is caused by the extremely LOR of the LCMO film, which obviously narrowed the space charge region in the LCMO film. The I - V behaviour of the Al/LCMO/Pt structure is also plotted in figure 1(a), which is obtained after a forming process. The extremely high resistance in positive scan and soft breakdown in negative scan, which is rather similar to that reported by Tsubouchi [15, 16] and opposite to that of the Ag TE reported previously [1, 2, 11, 13], implied the formation of an insulating layer (AlO_x) in the interface between the Al and LCMO films. We also examined the I - V behaviours of partial Al-50%Ag/LCMO/Pt units with HOR of 1–5 $\text{k}\Omega$. The percentage of these units is about 40%. The typical I - V characteristic indicated that a hysteresis phenomenon occurred clearly as shown in figure 1(b). It can be seen that the resistance decreased under the positive voltage sweep and increased under the negative voltage sweep. Both stable states are reversible and kept for long time. Compared with our previous report [3, 9, 11] and other reports [1, 2, 15, 16], it was found that the general trends of I - V curves from the structures with TEs of the Al-50%Ag alloy are similar to that of the Ag electrode and opposite to that of the Al electrode, meaning that the electron transport is carried by Ag in the Al-50%Ag electrode and the increase in the original resistance is induced by Al in it. So, this I - V characteristic can also be explained by carrier injected space charge limited conduction controlled by interface trapping/detrapping [3]. Otherwise, during the $0 \rightarrow +2\text{ V}$ scan, four ‘current leaps’ occur in the I - V curve at the start voltages of 1.4 V, 1.78 V, 1.93 V and 1.98 V, respectively. These ‘current leaps’ can be observed repeatedly in each $0 \rightarrow +2\text{ V}$ scan, implying that it is an intrinsic property of this sample. In addition, when the negative sweep voltage is in the range of about 1.7–1.9 V, the current starts to reduce with increasing voltage, called negative differential conductivity (NDC) phenomenon, which will vanish at the voltage beyond -1.9 V .

The EPIR change in HOR units was measured at room temperature as shown in figure 2. The positive pulse (current into the Al-50%Ag electrode) produced a decrease in resistance from the high-resistance state (HRS) to the low-resistance state (LRS), while a negative pulse (current into the Pt bottom electrode) caused an increase in resistance from the LRS to the HRS. After the forming process, stable bipolar switching was obtained. The average switching percentage of the resistance, defined as $R_S = 100 \times (R_H - R_L)/R_L$ (where R_H and R_L are the resistance at the HRS and the LRS, respectively), is around 120%, which can meet the need of practical applications for RRAM. But for pure Al and Ag electrodes, no stable EPIR switching can be acquired.

However, it is worth noting that the resistances of $\sim 60\%$ units in the Al-50%Ag TE sample are extremely low, about

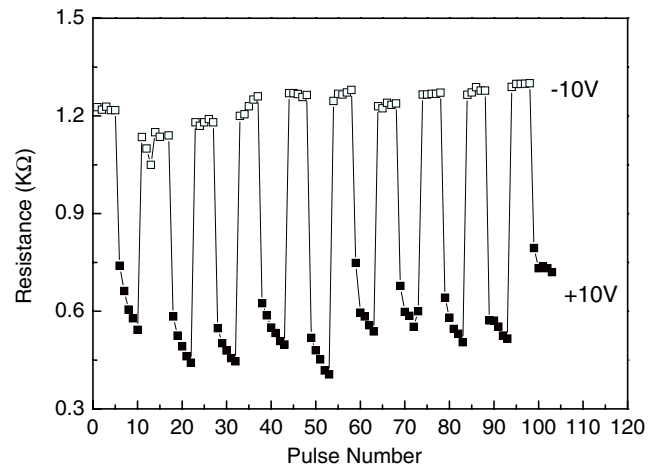


Figure 2. Electrical pulse induced resistive switching property of the Al-50%Ag/LCMO/Pt structure with an original resistance of 1.1 $\text{k}\Omega$.

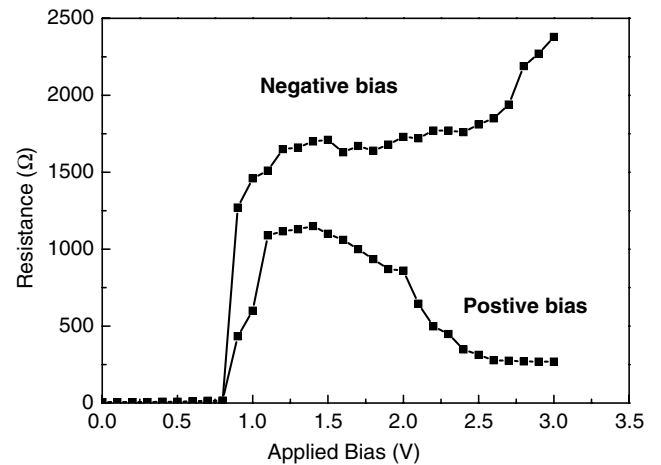


Figure 3. Resistances changes as a function of the positive and negative bias scans in extremely LOR Al-50%Ag/LCMO/Pt units.

6 Ω including the contribution of the Pt bottom electrode. This uneven original resistance distribution can also be found in the Al TE sample. An effective method was developed to increase the resistance of these extremely LOR units by a bias scan (see figure 3). Abrupt increases in the resistance were obtained at the bias of 0.9 V after both the positive and negative scans. The resultant resistances are 1.1–1.5 $\text{k}\Omega$, which are comparable to that of HOR units in HRS. With increasing scan bias beyond 1.4 V for positive scan and 2.7 V for negative scan, the resistances of the unit further increase under negative bias but decrease under positive bias, which corresponds to the EPIR characteristics of the LCMO film.

According to the deposition procedure, the overall cross-section of an objective unit can be divided into three layers: TE (Al, Ag, Al-50%Ag), LCMO film, BE (Pt). Firstly, it is necessary to understand the low-resistance origin of the LCMO film prepared in this work. By virtue of SEM and XRD analyses, we perceive that the low resistance of the LCMO film lies in the existence of the leakage channels, which is similar to that of ferroelectric thin films [20]. It can be deduced that there are two kinds of leakage channels in the LCMO

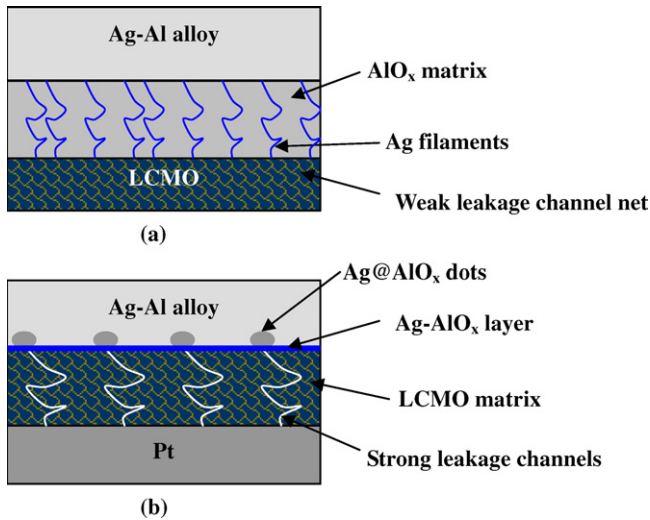


Figure 4. Schematic diagram of the interface layer between the Al–Ag alloy electrode and the LCMO film in HOR units (a) and extremely LOR units (b). The LCMO film in the HOR unit has a WLCN that results in a low resistance but the formation of Ag filaments in AlO_x increases its original resistance by point contact. Otherwise, the LCMO film in LOR unit has SLCs and a WLCN; the SLCs were blocked by Ag-contained AlO_x (Ag@AlO_x) dots formed during a bias scan.

(This figure is in colour only in the electronic version)

film, including a weak leakage channel net (WLCN) and strong leakage channels (SLCs), which will directly connect the TE and BE. The WLCN is inferred from the uniform low resistance of the pure Ag TE units, but the SLC is inferred from the uneven resistance distribution and the existence of extremely LOR units in Al and Al–50%Ag TE samples. Secondly, due to the low deposition temperature (200 °C), we believe that the Al–50%Ag TE layer has a uniform composition distribution and no second phase appeared. Finally, for Al metal and Al–50%Ag alloy TE, considering the strong oxidation properties of Al and the strong oxygen diffusion between Al and manganites [18], it is reasonable to assume that Ag contained AlO_x interlayers are formed between the Al–50%Ag TE and the LCMO film.

Based on the above descriptions of the LCMO film and the Al–50%Ag TE, we proposed a model to explain the switching of the Al–50%Ag TE sample. In the case of HOR units, due to the introduction of inert Ag, stable Ag conductive paths (filaments) will be created in the AlO_x matrix by a percolation effect (see figure 4(a)). The formation of Ag filaments results in the point contacts between Al–50%Ag TE and the LCMO film increasing the original resistances of these units, which is similar to that of the Ag paste sample [3, 9, 11]. The ‘current leaps’ in the positive I – V scan were produced by gradually turning on these Ag filaments. On the other hand, the NDC phenomena in the I – V curve of the Al–50%Ag TE only appeared at the negative scan rather than at the positive scan as shown in the first I – V cycle of the Al TE sample [10], which is also similar to that of the Ag paste sample [8]. This Ag-contained AlO_x layer can be formed by the oxidation of Al not only during the alloy electrode deposition but also during the electrical scan or applied pulse. Otherwise, the oxygen

in the LCMO interface region will be captured by Al in the TE, which can also result in the increase in the interface-region resistance in the LCMO film [21].

In the case of units with SLC-contained LCMO films and Al–50%Ag TE, only extremely LOR can be measured. After a bias scan, the SLCs were capped with Ag-contained AlO_x (Ag@AlO_x) dots as shown in figure 4(b). These dots were produced by a very large current density due to the huge conductive capability of the SLCs, which even induced the oxidation of Ag. In other words, large current (ampere order) flows mainly through the SLCs. The heat effect by this large current density (10^9 A cm^{-2} order) will promote the formation of a stable and insulative Ag@AlO_x dot. This blockage process is independent of the polarity of the scan bias, as shown in figure 3. After a scan treatment, the resistances of the extremely LOR units become comparable to that of the HOR units, and their subsequent switching process is also similar. These results also support the existence and blockage of the SLCs in extremely LOR units. The discussions about the formation of AlO_x in Al or Al–50%Ag TE in turn give possible evidence of the oxygen diffusion mechanism of the EPIR effect. However, on the basis of the discussion on the I – V characteristics of the Al–50%Ag TE HOR units, which is more similar to that of Ag TEs reported previously, we consider that the main mechanism dominating EPIR switching in our study is the trap-controlled SCLC process, but oxygen diffusion induces the formation of Ag-contained AlO_x to increase the original resistance of the Ag–50%Al TE units. Although the capability of the above model has been demonstrated, further investigation is needed to elucidate definitively the interface layer by structural and physical analysis methods and to investigate the effects of the Al and Ag ratios on the switching properties of LCMO films.

4. Conclusion

We have investigated the influence of TE materials on the resistance switching properties of a noncrystalline and low-resistance LCMO thin film. An Al–50%Ag alloy has been developed to realize the resistance switching of this low-resistance LCMO thin film. A model of the formation of Ag-contained AlO_x layer and insulative dots in the Al–50%Ag electrode was proposed to explain the characteristics of the Al–50%Ag TE sample, such as the derivation of LOR and HOR, the ‘current leap’ in I – V sweep, the abrupt resistance increase in the extremely LOR unit, and stable switching. The utilization of the Al–Ag alloy electrode will become an effective approach for improving the property uniformities of switching units by blocking the leakage channels in oxide films.

Acknowledgments

This work was sponsored by the Ministry of Science and Technology of China through the Hi-Tech Research and Development program of China (Grant No 2006AA03Z308) and the National Natural Science Foundation of China (No 50672116).

References

- [1] Liu S Q, Wu N J and Ignatiev A 2000 *Appl. Phys. Lett.* **76** 2749
- [2] Chen X, Wu N J, Strozier J and Ignatiev A 2005 *Appl. Phys. Lett.* **87** 233506
- [3] Shang D S, Wang Q, Chen L D, Dong R, Li X M and Zhang W Q 2006 *Phys. Rev. B* **73** 245427
- [4] Baikalov A, Wang Y Q, Shen B, Lorenz B, Tsui S, Sun Y Y, Xue Y Y and Chu C W 2003 *Appl. Phys. Lett.* **83** 957
- [5] Ouyang J Y, Chu C W, Szmanda C R, Ma L P and Yang Y 2004 *Nature Mater.* **3** 918
- [6] Rossel C, Meijer G I, Brémaud D and Widmer D 2001 *J. Appl. Phys.* **90** 2892
- [7] Zhuang W W *et al* 2002 *Tech. Dig.—Int. Electron Devices Meeting (San Francisco, CA)* p 193
- [8] Fujimoto M, Koyama H, Nishi Y and Suzuki T 2007 *Appl. Phys. Lett.* **91** 223504
- [9] Shang D S, Chen L D, Wang Q, Zhang W Q, Wu Z H and Li X M 2006 *Appl. Phys. Lett.* **89** 172102
- [10] Sawa A, Fujii T, Kawasaki M and Tokura Y 2004 *Appl. Phys. Lett.* **85** 4073
- [11] Dong R *et al* 2007 *Appl. Phys. Lett.* **90** 182118
- [12] Kim D S, Kim Y H, Lee C E and Kim Y T 2006 *Phys. Rev. B* **74** 174430
- [13] Odagawa A, Sato H, Inoue I H, Akoh H, Kawasaki M, Tokura Y, Kanno T and Adachi H 2004 *Phys. Rev. B* **70** 224403
- [14] Kim C J, Kim B I and Chen I W 2005 *Japan. J. Appl. Phys.* **44** 1260
- [15] Tsubouchi K, Ohkubo I, Kumigashira H, Oshima M, Matsumoto Y, Itaka K, Ohnishi T, Lippmaa M and Koinuma H 2007 *Adv. Mater.* **19** 1711
- [16] Harada T, Ohkubo I, Tsubouchi K, Kumigashira H, Ohnishi T, Lippmaa M, Matsumoto Y, Koinuma H and Oshima M 2008 *Appl. Phys. Lett.* **92** 222113
- [17] Shono K, Kawano H, Yokota T and Gomi M 2008 *Japan Soc. Appl. Phys.: Appl. Phys. Express* **1** 055002
- [18] Plecenik A, Frohlich K, Espinos J P, Holgado J P, Halabica A, Pripko M and Gilabert A 2002 *Appl. Phys. Lett.* **81** 859
- [19] Dong R, Wang Q, Chen L D, Shang D S, Chen T L, Li X M and Zhang W Q 2005 *Appl. Phys. Lett.* **86** 172107
- [20] Damjanovic D 1998 *Rep. Prog. Phys.* **61** 1267
- [21] Nian Y B, Strozier J, Wu N J, Chen X and Ignatiev A 2007 *Phys. Rev. Lett.* **98** 146403